

Neurotoxicity of Silica Nanoparticles: Brain Localization and Dopaminergic Neurons Damage Pathways

Jie Wu, Chen Wang, Jiao Sun,* and Yang Xue

Shanghai Biomaterials Research & Testing Center, Shanghai Key Laboratory of Stomatology, Ninth People's Hospital, Shanghai Jiaotong University School of Medicine, Shanghai 200023, China

Because of the unique physicochemical properties such as small size, large surface area, high reactivity, and high drug loading efficiency, silica nanoparticles (SiO_2 -NPs) have been developed for mechanical polishing, additives to food and cosmetics, and various applications in biomedical fields, including optical imaging, cancer therapy, targeted drug delivery, and controlled drug release for genes and proteins.^{1–4} Such wide applications have also raised concerns with the safety of SiO_2 -NPs when they are released into the environment and in human tissues, especially occupational exposure at manufacturing premises. This may pose a health threat because studies have reported that SiO_2 -NPs might adversely affect cell function through producing a great amount of reactive oxygen species (ROS) and triggering apoptosis or proinflammatory responses in different types of cultured cells such as human lung cancer cells,⁵ mouse peritoneal macrophages,⁶ human lymphoblastoid cells,⁷ human umbilical vein endothelial cells,⁸ and microglia.⁹ The evidence obtained from animal models has concluded that SiO_2 -NPs could elicit moderate to severe pulmonary inflammation.¹⁰ Recent *in vivo* studies from our laboratory using radioactive iodine labeling and radioactivity counting found that SiO_2 -NPs were accumulated mainly in the liver and spleen and subsequently caused hepatocyte necrosis at the portal triads.¹¹ However, so far there is a lack of information concerning the potential hazards of SiO_2 -NPs to the brain.

Existing research has shown that quantum dots,¹² single-walled carbon nanotubes,¹³ and other nanomaterials were capable of crossing the blood-brain barrier (BBB) and entered the brain. It has been reported that titanium dioxide¹⁴ and manganese

ABSTRACT Silica nanoparticles (SiO_2 -NPs) are being used increasingly in diagnosis, imaging, and drug delivery for the central nervous system. However, to date, little is known concerning the potential adverse effects on the brain associated with exposure to SiO_2 -NPs. The present study was conducted to trace, locate, and quantify SiO_2 -NPs in the brain by a radiolabeling approach after intranasal instillation with SiO_2 -NPs. The oxidative stress, inflammatory response, and levels of neurochemicals in the brain were also analyzed. Furthermore, *in vitro* studies were carried out to elucidate the pathway and mechanism of *in vivo* damage with a co-incubation model of dopaminergic neuron PC12 and SiO_2 -NPs. The results indicated that SiO_2 -NPs *via* intranasal instillation entered into the brain and especially deposited in the striatum. Exposure to SiO_2 -NPs also induced oxidative damage and an increased inflammatory response in the striatum. Meanwhile, results of *in vitro* studies demonstrated that exposure to SiO_2 -NPs decreased cell viability, increased levels of lactate dehydrogenase, triggered oxidative stress, disturbed cell cycle, induced apoptosis, and activated the p53-mediated signaling pathway. In addition, the *in vivo* injury of neurochemicals occurred as the SiO_2 -NPs appeared to induce depleted dopamine in the striatum, and the down-regulation of tyrosine hydroxylase protein was the main contribution. These data demonstrate that SiO_2 -NPs possibly have a negative impact on the striatum and dopaminergic neurons as well as a potential risk for neurodegenerative diseases. There is potential concern with SiO_2 -NPs' neurotoxicity in biomedical applications and occupational exposure in large-scale production.

KEYWORDS: silica nanoparticles · neurotoxicity · biodistribution · oxidative stress · dopamine · neurons

oxide¹⁵ nanoparticles were capable of translocating along the olfactory nerve pathway to the brain after intranasal instillation exposure, accumulating in the olfactory bulb, cortex, and cerebellum. Moreover, the deposition in the brain of nanoparticles such as ferrous oxide¹⁶ and carbon black¹⁷ can stimulate oxidative stress, inflammatory responses, and pathological changes. These observations have provided the evidence that nanoparticles can not only reach the brain but also cause a certain degree of brain tissue damage. Therefore, it is of interest whether SiO_2 -NPs translocate to the brain and induce consequential side effects in the brain.

Brain tissue is composed of two main cell types: neurons and glial cells. Neurons are

* Address correspondence to jiaosun59@yahoo.com.

Received for review December 20, 2010 and accepted April 28, 2011.

Published online April 28, 2011
10.1021/nn103530b

© 2011 American Chemical Society

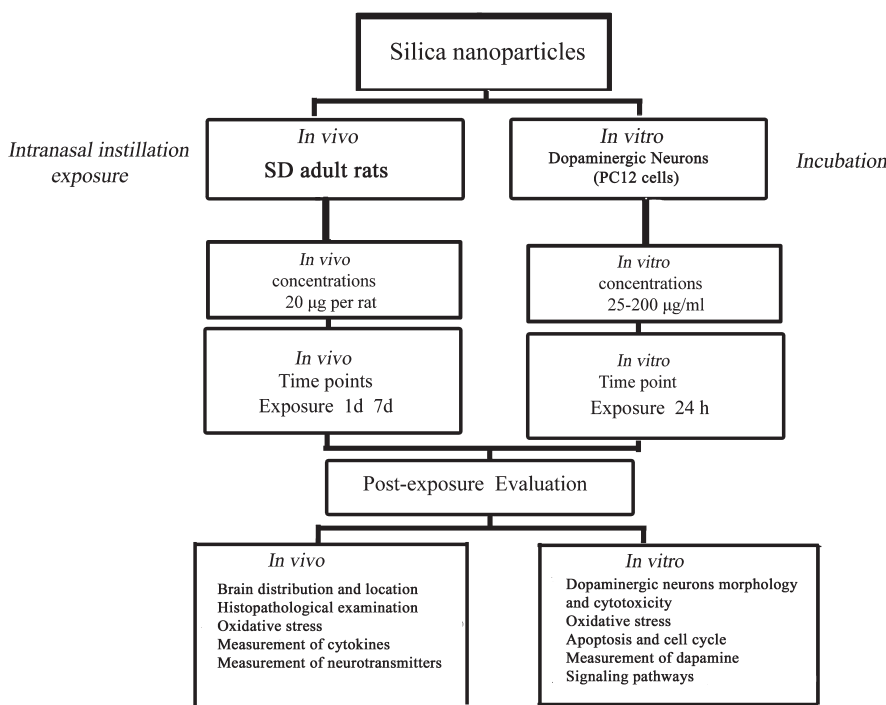


Figure 1. Experimental design for *in vivo* and *in vitro* experiments.

the core components of the brain and are critical for the maintenance of brain function. The damage of neurons such as loss of structure or function was considered to play essential roles in the etiology of certain neurodegenerative diseases including Hallervorden–Spatz syndrome, Parkinson's disease, and Alzheimer's diseases.¹⁸ There have been a limited number of studies that observed the potential neurotoxicity of nanoparticles on neurons. For instance, Pisanic *et al.*¹⁹ showed that the exposure to anionic magnetic nanoparticles (MNPs) induced a dose-dependent decrease in the viability of PC12 cells (a paradigm for dopaminergic neuron) and the capacity to extend neurites in response to nerve growth factor (NGF). Hussain *et al.*²⁰ reported that the increased production of ROS caused by manganese oxide (Mn-40 nm) particles was attributed to the depletion of dopamine (DA) in PC12 cells; however, precise neuron damage pathways and mechanisms induced by nanoparticles remain ill-defined.

In the present study, we utilized a stable isotopic tracing approach based on our published method¹¹ to detect the distribution, localization, and accumulation of SiO₂-NPs in the brain after intranasal instillation and consequently to estimate the potential particle-induced injuries and function alterations in the brain. According to the outcomes of localization *in vivo*, we conducted *in vitro* studies wherein SiO₂-NPs were incubated with dopaminergic neuron PC12.²¹ Through the changes in cell viability, oxidative stress, cell cycle, apoptosis, dopamine content, and cell signaling pathway, we further investigated the pathways and mechanism of *in vivo* and *in vitro* damage.

RESULTS AND DISCUSSION

While the beneficial aspects of SiO₂-NPs are widely publicized, some new concerns have arisen including the negative impact of SiO₂-NPs on living cells and lung tissue. However, there are still many unknowns such as whether SiO₂-NPs enter the brain and exert adverse effects on the brain and how SiO₂-NPs interact with the brain tissues and neurons. The present study attempts to answer some of these questions using the experimental protocol illustrated in Figure 1.

Characterization, Identification, and Stability of SiO₂-NPs and ¹²⁵I-SiO₂-NPs. The SiO₂-NPs employed in this study were 15 nm in size measured by TEM (Figure 2A). To understand the state of dispersion of SiO₂-NPs when put into physiological saline and high-glucose DMEM containing 10% FBS, the SiO₂-NPs samples were analyzed by dynamic light scattering (DLS). The DLS results showed agglomeration of the SiO₂-NPs approximately 10 times their primary particle size at 156 nm in physiological saline and 6 times greater than their primary size at 92 nm in DMEM cell culture medium (Figure 2C). Current evidence implied that agglomeration of nanoparticles is likely to affect their toxicity in biological systems in a variety of ways, such as cellular uptake, distribution *in vivo*, sedimentation rate, and even ROS production.²² The findings of several studies indicated that the nanotoxicity is depressed by the agglomeration of nanoparticles,^{22,23} whereas results of others suggested that the agglomeration of nanoparticles could pose a greater hazard than the well-dispersed samples. Therefore, it is necessary to systematically and

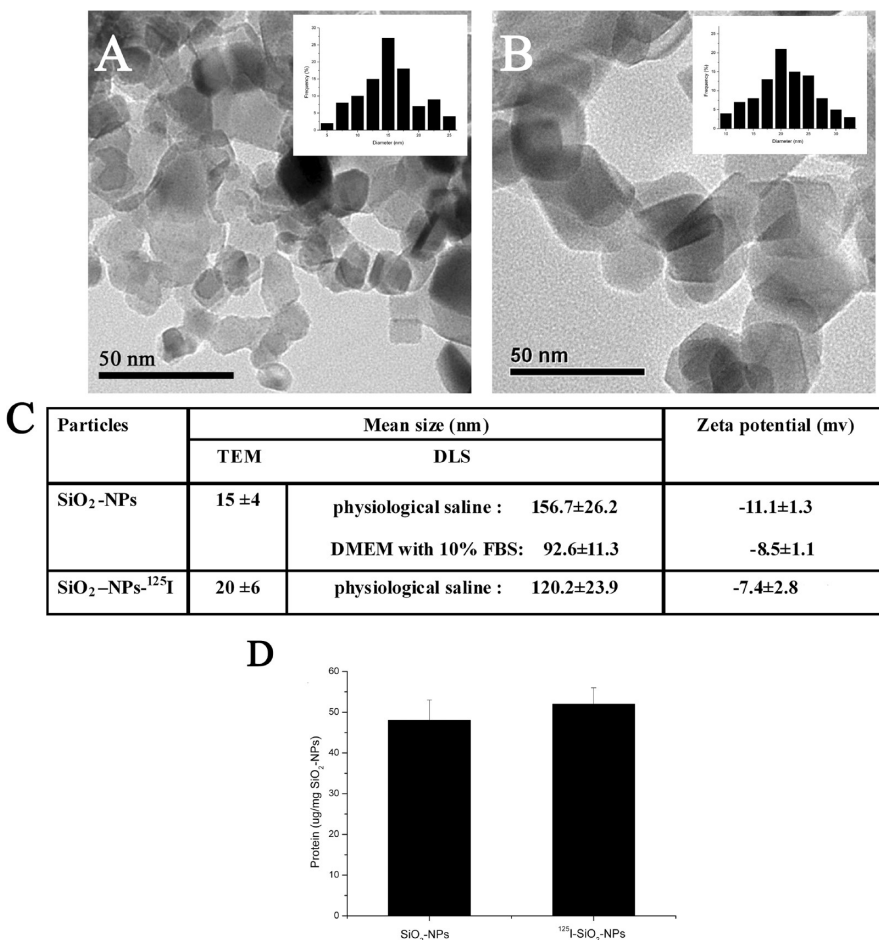


Figure 2. Characterization of SiO₂-NPs and ¹²⁵I-SiO₂-NPs. (A) TEM analysis of SiO₂-NPs. **(B)** TEM analysis of ¹²⁵I-SiO₂-NPs. **(C)** Particle size, hydrodynamic diameter, and zeta potential. **(D)** Amount of rat serum protein adsorbed on the SiO₂-NP and ¹²⁵I-SiO₂-NP surfaces. Inset plots in A and B demonstrate the particle size distribution from TEM observations of samples A and B, respectively. FBS: fetal bovine serum.

accurately define particle characteristics in order to understand the potential toxicity of nanoparticles to biological systems to ensure that results are reproducible.²² There is also a need to take into account the roles of properties other than size such as pH or surface charge in the toxicity of the SiO₂-NPs in future studies.

To answer the question of whether the SiO₂-NPs could exert toxic effects on the brain, we needed first to know the distribution of SiO₂-NPs in the brain. Unfortunately, at present there is no ideal method for tracing and quantifying SiO₂-NPs in the brain. To date, *in vivo* distribution studies have used the methods of fluorescence,²⁴ ICP-MS,¹⁴ and ICP-AES.²⁵ Fluorescence detection provides the advantage of visual evaluation; however, it reflects only a semiquantitative assessment and is easy to quench. Although the method of ICP-MS has been used for quantitation studies, the detection of nanoparticles would be hampered by the natural presence of endogenous elements in the tissues. Isotope tracer technique has been widely applied in the areas of drug metabolism and medical diagnosis. It offers many advantages for monitoring purposes in the

nanotoxicology field including (a) quantitative data; (b) long-term evaluation; (c) fully reflecting the existence of nanoparticles; and (d) avoiding influence of the element background in the brain. A recent study in our laboratory labeled the SiO₂-NPs with radioactive iodine (¹²⁵I) and used a γ -counter to assess quantitatively the tissue distribution of SiO₂-NPs in mice up to 30 days.¹¹ The results revealed that the analytical method of radioactive counting was appropriate and adequate for the detection and localization of nanoparticles *in vivo*.

In order to accomplish the radiolabeling, the SiO₂-NPs were first required to be modified with aminopropyltriethoxysilane (APTS) to introduce amino groups on their surface. As shown in Figure 3A, after surface modification with APTS, the characteristic absorption peaks of both SiO₂-NPs (1080 cm^{-1}) and APTS (785, 1630, and 2886 cm^{-1}) emerged in the SiO₂-NPs samples, indicating that the APTS had successfully modified the surface of SiO₂-NPs and did not influence the particles' structure. The presence of the ¹²⁵I tag might alter the original characteristic of the nanoparticles, subsequently changing the biodistribution and

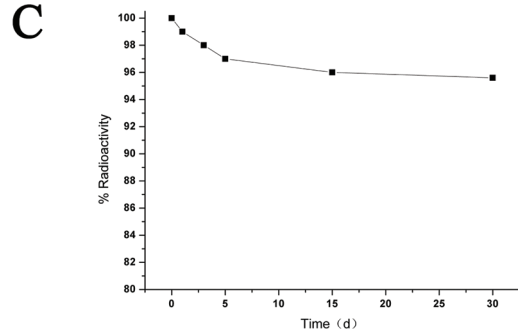
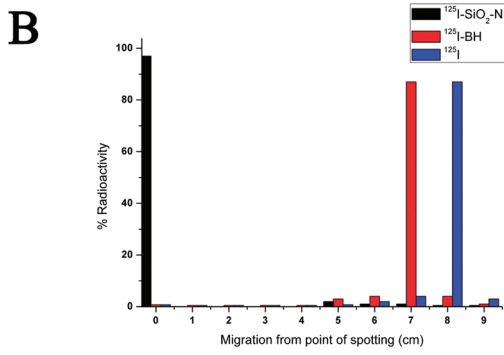
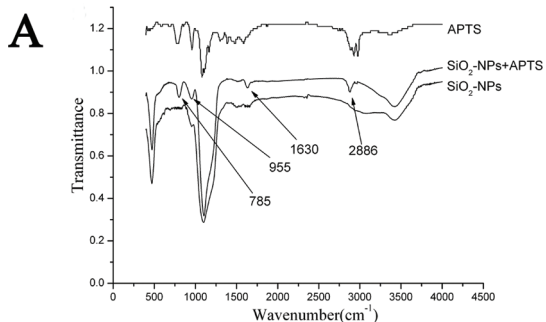


Figure 3. Identification and stability of ^{125}I -SiO₂-NPs: (A) FTIR spectra of ^{125}I -SiO₂-NPs; (B) identification of ^{125}I -SiO₂-NPs by ITLC-SG; (C) stability of ^{125}I -SiO₂-NPs.

clearance.²⁶ However, our results demonstrated that the shape of SiO₂-NPs labeled with ^{125}I was spherical, consistent with the original shape (Figure 2B). No significant increase in size occurred in the labeled particles (Figure 2C). The results of zeta potential determination showed that ^{125}I -SiO₂-NPs still maintained a negative surface charge (Figure 2C). Figure 2E presents the amount of adsorbed proteins on the SiO₂-NPs and ^{125}I -SiO₂-NPs from rat serum. The group of ^{125}I -SiO₂-NPs showed a slightly higher protein adsorption than that of the SiO₂-NPs group, but there were no significant differences. The serum proteins binding on the nanoparticle surface would influence the biobehavior of particles in the body, through being recognized by the scavenger receptors on the phagocyte cell surface and internalized, leading to an obvious loss of nanoparticles from the circulation.²⁷ Due to the negatively charged serum proteins, a tendency was observed that the lower zeta potential obtained, the lower amount of adsorbed protein. Our results found that the adsorption of protein onto the native and

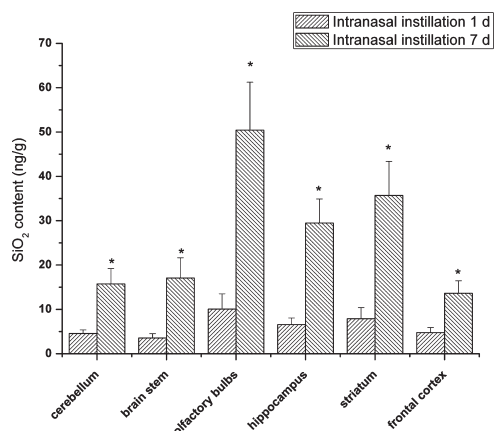


Figure 4. SiO₂-NP content in the rat brains ($n = 6$) after intranasal instillation with SiO₂-NPs at time points of 1 day and 7 days. * $p < 0.05$ when compared with the 1-day group.

radiolabeled nanoparticles had no effect, implying that the ^{125}I tag did not significantly alter the biological reaction of SiO₂-NPs in the body.

Radiochemical purity and an excellent stability of radiolabeling are important for the accuracy of the results. In our study, the labeling yield and purity of the ^{125}I -SiO₂-NPs were determined by paper chromatography using instant thin-layer chromatography–silica gel (ITLC-SG). As shown in Figure 3B, ^{125}I moved toward the solvent front ($R_f = 0.8$) faster than ^{125}I -BH ($R_f = 0.7$), but the ^{125}I -SiO₂-NPs remained at the point of spotting ($R_f = 0$) with the labeling yield reaching 95%. Additionally, as shown in Figure 3C the ^{125}I -SiO₂-NPs were stable for 30 days *in vitro*, and the purity was consistently greater than 95% at all times. Therefore, the above results indicated that the product obtained from radioactive iodine labeling was of high purity and good stability, which laid the foundation for the *in vivo* tracing research.

Biodistribution, Localization, and Accumulation Studies.

The first and most important step in assessing the neurotoxicity of SiO₂-NPs is to determine their fate in the brain. In the present study, intranasal instillation of SiO₂-NPs for 1 day and 7 days resulted in a significant increase in SiO₂-NP content in the brain, and the ranking of SiO₂-NP levels in sub-brain regions was olfactory bulb > striatum > hippocampus > brain stem > cerebellum > frontal cortex (Figure 4). Several studies have described that the olfactory nerve pathway is an important route for translocating inhaled or intranasal instilled nanoparticles to the brain bypassing the BBB.^{14,15} Except for the olfactory bulb, the striatum appeared to be the major accumulation site of intranasal instillation of SiO₂-NPs (Figure 4). As a crucial component of the brain, the striatum plays essential roles in the modulation of movement pathways and appears closely related to neurodegenerative disorders such as Parkinson's disease.²⁸ Moreover, we also found that the SiO₂-NP content in the hippocampus

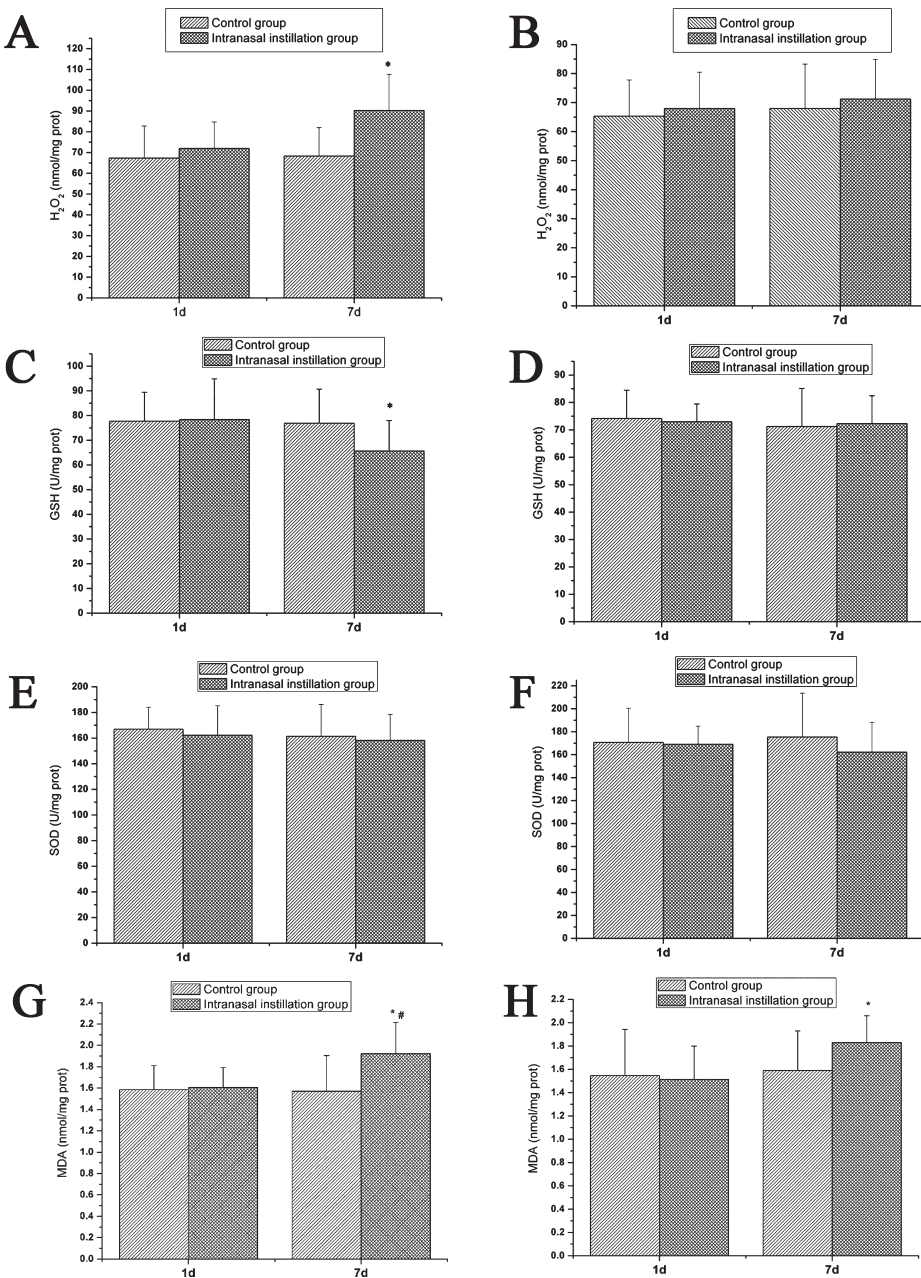


Figure 5. Changes in H_2O_2 , GSH, SOD, and MDA levels in the hippocampus and striatum of rats ($n = 6$) intranasally instilled with physiological saline and SiO_2 -NPs at the time point of 1 day and 7 days. (A, C, E, and G) H_2O_2 , GSH, SOD, and MDA levels in the striatum. (B, D, F, and H) H_2O_2 , GSH, SOD, and MDA levels in the hippocampus. * $p < 0.05$ when compared with control, # $p < 0.05$ when compared with 1 day group.

was second to that in the striatum (Figure 4). The hippocampus is responsible for learning and long-term memory, and in Alzheimer's disease, the hippocampus is one of the first regions of the brain to suffer damage.²⁹ Therefore, these results suggest that it is imperative to determine whether the exposure to SiO_2 -NPs could induce potential injuries in the striatum and hippocampus, which would increase the risk of developing neurodegenerative disorders.

General Behavior Observation. In the experimental and control groups, no changes in general behavior were detected in the rats administered SiO_2 -NPs ($n = 6$) and

physiological saline ($n = 6$). The results suggest that intranasally instilled SiO_2 -NPs for 1 day and 7 days at a relatively low dose (20 $\mu\text{g}/\text{d}$) do not cause disorders in general behavior. However, the more extensive and in-depth neurobehavioral examination involving a rotation test, open field test, and water maze test should be considered in further studies to better elucidate the neurotoxicity of SiO_2 -NPs.

Oxidative Damage and Inflammatory Responses in the Rat

Brain. The time-course changes of H_2O_2 , GSH, SOD, and MDA levels are presented in Figure 5. The striatum exhibited a greater vulnerability to oxidative stress,

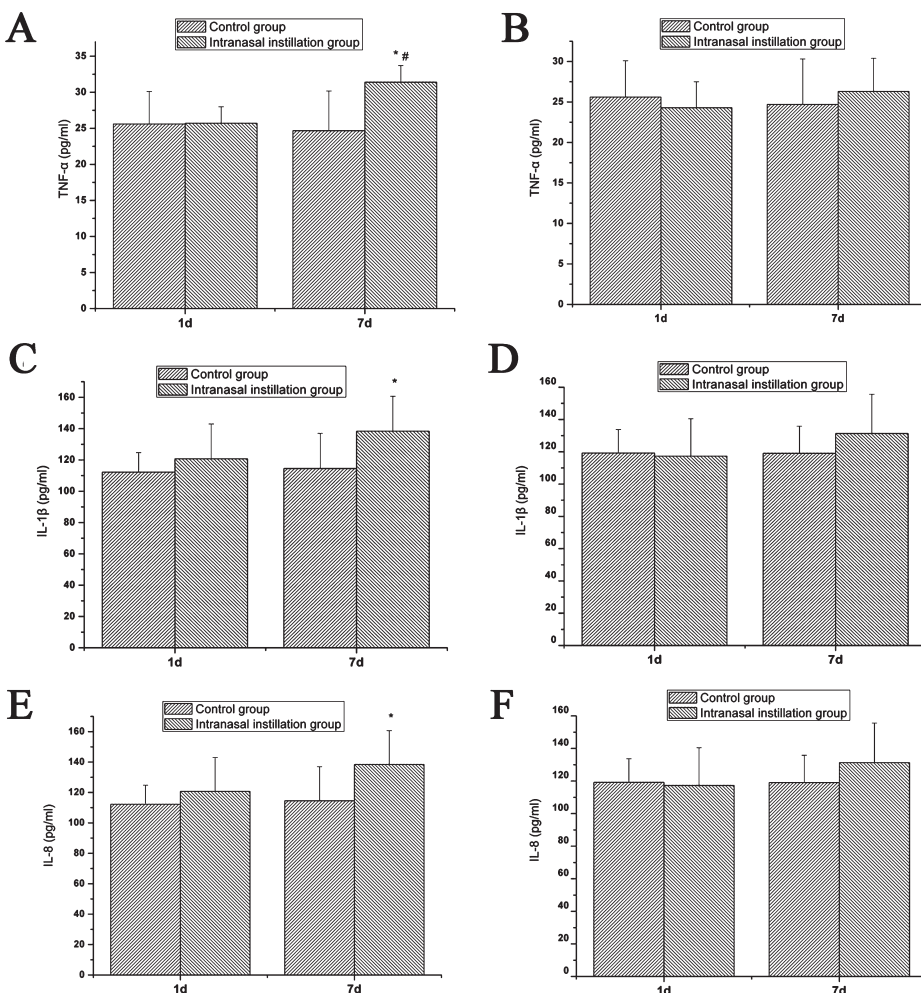


Figure 6. Levels of TNF- α , IL-1 β , and IL-8 in the hippocampus and striatum of rats ($n = 6$) intranasally instilled with physiological saline and SiO₂-NPs at the time point of 1 day and 7 days. (A, C, and E) TNF- α , IL-1 β , and IL-8 levels in the striatum. (B, D, and F) TNF- α , IL-1 β , and IL-8 levels in the hippocampus. * $p < 0.05$ when compared with control, # $p < 0.05$ when compared with 1-day group.

with an apparent elevation in H₂O₂ and MDA levels and a significant decrease in the GSH activity when compared to the control at the time point of 7 days ($p < 0.05$). H₂O₂, a metabolic byproduct of ROS, is capable of activating the transcription factor NF- κ B and has been implicated in certain neurodegenerative diseases. GSH is a key antioxidant in the body that plays crucial roles in maintaining the stability of cellular redox status. Excessive radicals react with the cell membrane, which consists mainly of lipids, and finally lead to lipid peroxidation. MDA is the end product and detection index of lipid peroxidation. The results obtained in the present study showed that SiO₂-NPs deposited in the striatum may induce oxidative damage. Prolonged and serious oxidative stress possibly contributes to the inflammatory process by activating inflammation-related genes and transcription factors such as NF- κ B and AP-1.³¹ To further evaluate the inflammatory response by SiO₂-NPs, TNF- α , IL-1 β , and IL-8 were chosen as the indicators of inflammatory response. Significantly high TNF- α and IL-1 β levels ($p < 0.05$) induced by exposure to SiO₂-NPs for 7

days were observed in the striatum (Figure 6A,B). However, there was no significant change in IL-8 levels (Figure 6C). The contribution of oxidative stress after translocation to the brain could activate the microglia, astrocytes, and endothelial cells to release pro-inflammatory cytokines such as TNF- α and IL-1 β , which further stimulate the expression of IL-6 and IL-8.³² Several studies have confirmed that inflammation can play a causal role in dopaminergic neuron death and is involved in the pathological process of some neurodegenerative diseases.³³ In the current study, SiO₂-NP-induced damage in the brain was possibly caused by toxic effects of oxidative stress and inflammatory mediators.

Nevertheless, except for MDA, there are no obvious changes in the other three markers of oxidative stress and inflammation response in the hippocampus (Figures 5 and 6), which was possibly due to the lower content of SiO₂-NPs in the hippocampus, resulting in relatively weak oxidative injuries.

Pathology Changes. Histopathological analyses of the brain revealed that intranasal instillation exposure to

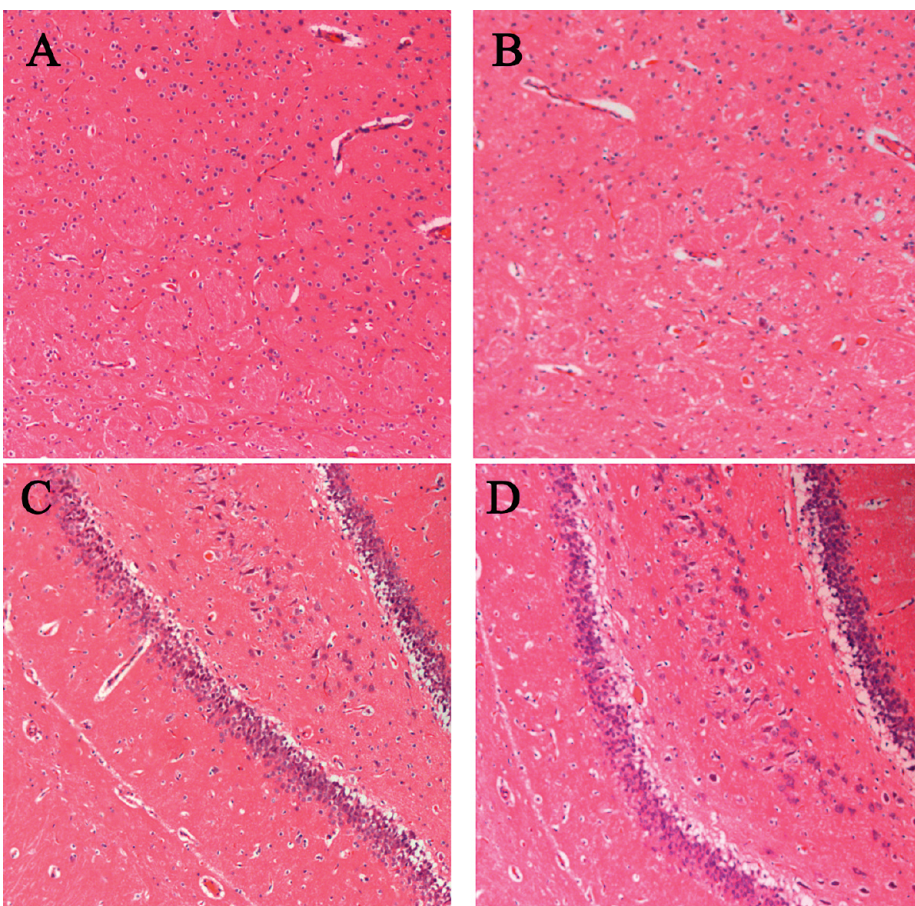


Figure 7. Histopathology of the rat brain tissue after intranasal instillation with SiO_2 -NPs and physiological saline at the time point of 7 days. (A) Control group of striatum region. (B) SiO_2 -NP group of striatum region. (C) Control group of hippocampus region. (D) SiO_2 -NP group of hippocampus region. Sections were stained with H&E and observed under a light microscope at 10 \times magnification.

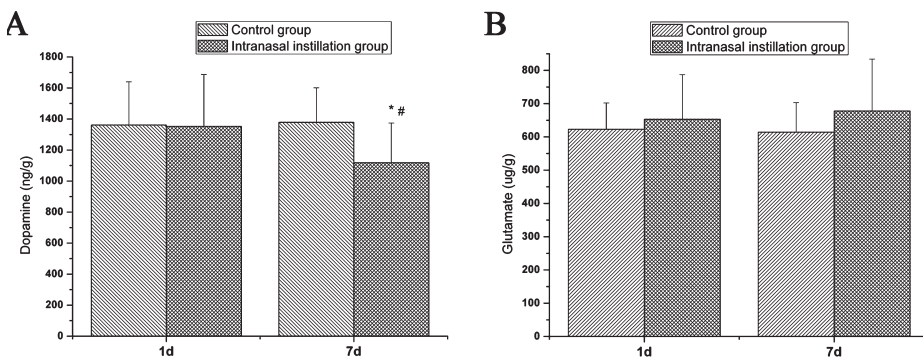


Figure 8. Changes of dopamine levels in the striatum (A) and glutamate levels in the hippocampus (B) after intranasal instillation with physiological saline and SiO_2 -NPs at the time point of 1 day and 7 days. $N = 6$, * $p < 0.05$ when compared with control, # $p < 0.05$ when compared with 1-day group.

SiO_2 -NPs produced no apparent changes in the histology of the brain when compared with the physiological saline-exposed controls (Figure 7). We speculate that the weak reaction in oxidative stress and slight increase in cytokines, which are some of the biochemical markers of early brain damage, did not affect the cellular integrity and tissue morphology. Wang *et al.*³⁰ also found no abnormal pathology changes in the heart,

lung, testicle (ovary), and spleen tissues two weeks after a single oral administration of TiO_2 nanoparticles (25 and 80 nm), although some serum biochemical parameters such as LDH were observed to be higher than in the control group.

Influence on the Neurochemicals in the Brain. While we discovered that SiO_2 -NPs caused oxidative stress and inflammation in the striatum, it was still unclear

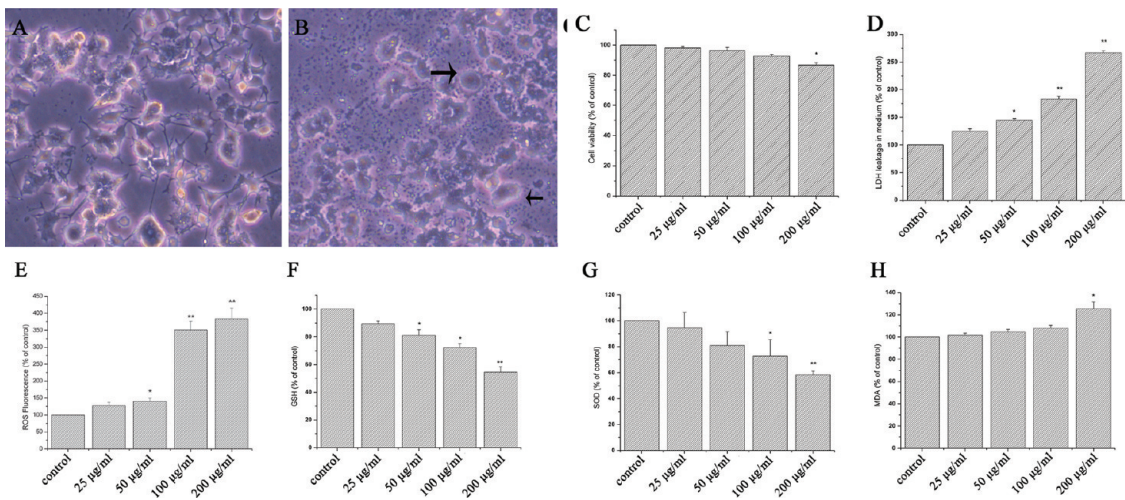


Figure 9. Morphological characterization of PC12 cells and effects of SiO₂-NPs on viability, LDH levels, and oxidative stress of PC12 cells. (A) PC12 cells without any nanoparticle treatment (10 \times). (B) PC12 cells treated with SiO₂-NPs (200 μ g/mL, 10 \times). (C) Viability of PC12 cells treated with SiO₂-NPs for 24 h as measured by the MTS assay. (D) LDH level of PC12 cells cultured in media containing SiO₂-NPs for 24 h. (E) ROS production (6 h incubation time) after treatment with SiO₂-NPs. (F, G, and H) Levels of GSH, SOD, and MDA (24 h incubation time) after treatment with SiO₂-NPs. $N = 3$, * $p < 0.05$ when compared with control, ** $p < 0.01$ when compared with control. Arrow: cells with rounded shapes and reduced length of extended neurites.

whether the damage would affect the striatal function. The release of neurotransmitters is critical for normal brain functions. Dopamine (DA) is a major neurotransmitter in neural systems innervating the striatum and is thought to play an important role in motivation, by attaching cognition of incentive significance to stimuli. The results of the high-performance liquid chromatography (HPLC) assay (Figure 8A) indicated that, with the time prolonged, a significant reduction of DA activity in the striatum was observed ($p < 0.05$). Animal models revealed that the DA depletion in the striatum consequently resulted in movement disorders that were characterized by Parkinson's disease.³² Thus, the reduction of DA confirmed the changes of brain function caused by SiO₂-NPs, indicating potential risk factors for developing Parkinson's disease. Glutamate (Glu) is the most common excitatory neurotransmitter in the brain and is considered to be involved in cognition, memory, and learning. In the present study, the Glu content in the hippocampus from the 7-day exposure groups was slightly higher than that in the control group, but there were no significant differences between them, indicating that SiO₂-NPs may have minimal effect on the secretion of Glu in the hippocampus. However, further investigations on long-term exposure and other parts of the brain are necessary, as memory and motivation are complex neural pathways and processes that require the coordination and cooperation of many different regions and neurotransmitter systems of the brain.

Cell Morphology, Dose-Dependent Cytotoxicity, and Oxidative Stress. To explicate the mechanism of striatum injury, PC12 cells were selected as the model for the studies at the cellular and molecular levels. The PC12 cell is a cell line derived from rat adrenal medulla pheochromocytoma. Differentiated PC12 cells induced by NGF have

typical characteristics of dopaminergic neurons in form and function and widely serve as a paradigm for neurobiological studies.²¹ PC12 cells were exposed to SiO₂-NPs for 24 h, and the morphological changes were examined using a phase-contrast microscopy. Following exposure to NGF, as shown in Figure 9A, PC12 cells differentiated into neuronal type cells and began to extend neurites into their periphery. However, as shown in Figure 9B, after exposure with 200 μ g/mL of SiO₂-NPs for 24 h, some PC12 cells appeared to become rounder and have a reduction in their ability to generate neurites following NGF induction. This could be caused by a disorder in cytoskeletal structure as a consequence of nanoparticle treatment. Similar results were reported in other groups, such as PC12 cells treated with magnetic nanoparticles¹⁹ and human glioblastoma cells (U251) treated with silver nanoparticles.³⁴

Cytotoxicity is a vital step in toxicology that detects cellular responses to a toxicant. In the current study, cytotoxicity in response to different concentrations of SiO₂-NPs presented in the culture medium was evaluated by MTS and LDH assays, which reflect the mitochondrial function in living cells and membrane integrity, respectively. Figure 9C shows that, after exposing PC12 cells to SiO₂-NPs for 24 h, cell viability decreased to 86.72% at the highest concentration (200 μ g/mL), which was significantly lower than that of the control ($p < 0.05$). Furthermore, when incubated at the lower concentration of 50 μ g/mL, the LDH release was obviously elevated (Figure 9D). We speculate that SiO₂-NP-induced membrane damage is more severe than the changes in mitochondrial enzyme activity. Cell-membrane disruption can lead to irreversible cell degeneration, ultimately resulting in cell swelling and death.

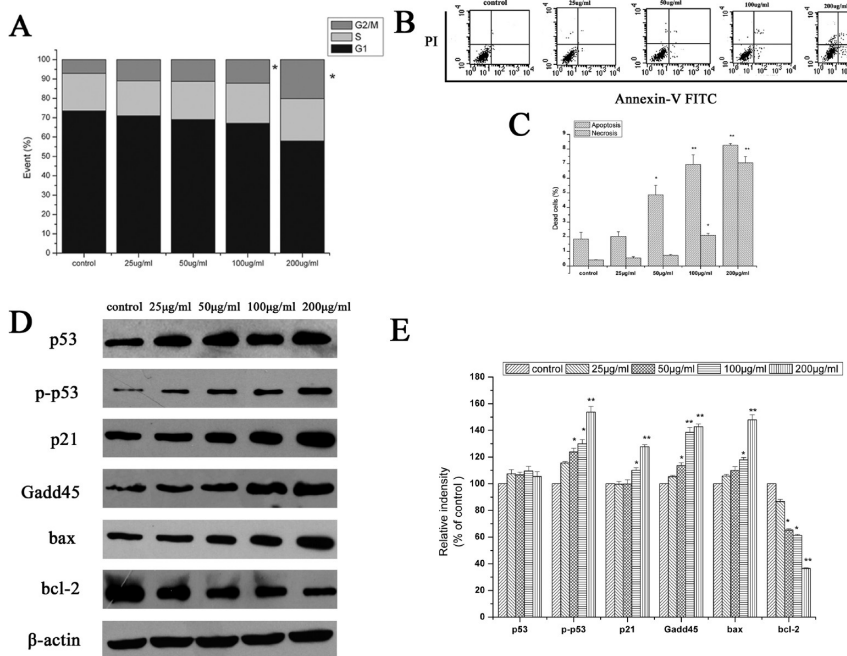


Figure 10. Analysis of cell cycle, apoptosis, and molecular mechanism of SiO₂-NP-treated PC12 cells. (A) Cell cycle distribution of PC12 cells cultured with SiO₂-NPs. (B and C) Apoptosis and cell death induced by SiO₂-NP treatment in PC12 cells double-stained with PI- and FITC-labeled annexin V. (D) Western blot analysis of p53, p-p53, p21, Gadd45, bax, and bcl-2 expression in PC12 cells induced by SiO₂-NPs. (E) Densitometry showing data from three experiments. $N = 3$, * $p < 0.05$ when compared with control, ** $p < 0.01$ when compared with control.

To further interpret the injury process, as shown in Figure 9 (E–H), the cytotoxicity was examined in accordance with the intracellular oxidative stress levels measured by GSH depletion, MDA production, SOD inhibition, and ROS generation. The findings confirmed the *in vivo* results and also indicated that oxidative stress might be a key route in the cytotoxicity of SiO₂-NPs. The literature has documented that ROS and oxidative stress are valid criteria for evaluating the toxicity of nanoparticles, as both play important roles in the induction of nanoparticle-associated injuries.³⁵ It is noteworthy that SiO₂-NPs can easily induce oxidative stress in the brain *in vivo* and in PC12 cells *in vitro*. It is well-documented that the brain tissue is vulnerable to oxidative damage because of its high metabolic rate, cellular content of lipids and proteins, low levels of endogenous scavengers, and extensive axonal and dendritic networks.³⁶ Studies conducted by our team have found that, at a dose of 100 μg/mL, SiO₂-NPs can induce significant generation of ROS in human umbilical vein endothelial cells,⁸ whereas in the present study, at the lower concentration of 50 μg/mL, the neuron cells show obvious ROS production (Figure 9E). The results demonstrate that very small doses of SiO₂-NPs may cause significant oxidative stress in brain tissues. There has been an increase in biochemical, clinical, and epidemiological data that indicate the association of excessive ROS generation with various diseases, such as cancer, aging, and most neurodegenerative disorders.^{37,38} Our findings reveal the potential

risk for the application of SiO₂-NPs, especially for the brain, which is susceptible to oxidization. Highly reactive molecules such as ROS could also react unfavorably with cellular macromolecules including DNA. ROS-induced DNA damage is typified by single- and double-stranded DNA breaks and base modifications, resulting in cell cycle arrest and even mutations.³⁹ In order to determine whether the SiO₂-NPs exert the same effect on neurons, we further investigated changes in the cell cycle in PC12 cells, as described below.

Effect of SiO₂-NPs on Cell Cycle and Apoptosis and the Involved Mechanism. Cell cycle analyses of PC12 cells with SiO₂-NP treatment are shown in Figure 10A. SiO₂-NPs induced significant accumulation in the G2/M phase at a concentration of 100 and 200 μg/mL compared to the control ($p < 0.05$). Excessive generation of ROS can adversely affect the permeability of the mitochondrial membrane, damage the respiratory chain, and cause DNA damage, where early effects become evident in the cell cycle progression.⁴⁰ In our study, G2/M cell cycle arrest could inhibit cell proliferation, while it could also provide enough time for the cells to repair the damaged DNA; however, if a cell is no longer capable of effectively repairing the damage incurred to its DNA, it may enter a state of apoptosis, evoking arrested cells irreversibly in the G2/M phase. This assumption is supported by the results presented in Figure 10 (B and C). When the cells were treated with SiO₂-NPs, the numbers of apoptosis cells increased markedly from the dose of 50 μg/mL.

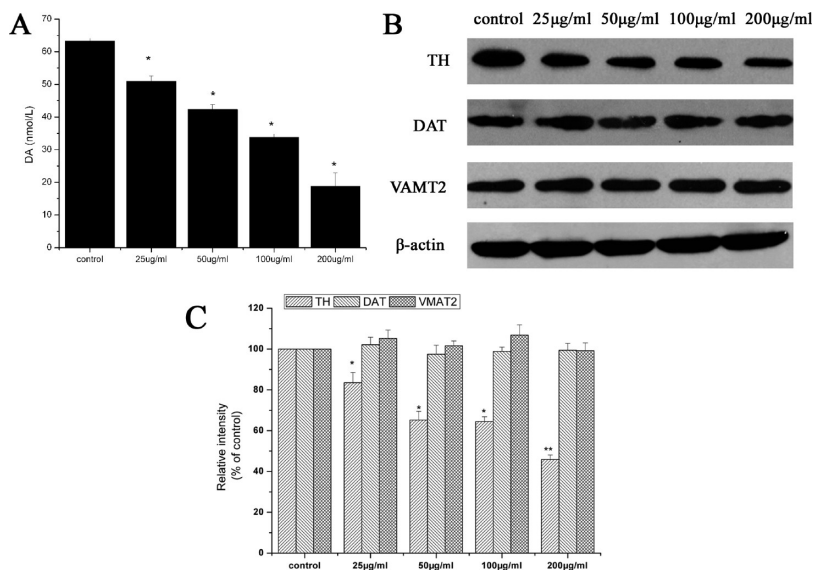


Figure 11. Analysis of DA content and molecular mechanism of SiO₂-NPs-treated PC12 cells. (A) DA content of PC12 cells cultured with SiO₂-NPs. **(B)** Western blot analysis of TH, DAT and VMAT2 expression in PC12 cells induced by SiO₂-NPs. **(C)** Densitometry showing data from three experiments. $N = 3$, * $p < 0.05$ when compared with control, ** $p < 0.01$ when compared with control.

To explore the possible molecular mechanisms of SiO₂-NP-mediated apoptosis and cell cycle arrest, we measured the expression levels of regulators involved in the apoptosis pathway and G2/M DNA damage checkpoint. As shown in Figure 10 (D and E), p53 phosphorylation increased in a dose–response manner in PC12 cells that had been exposed to SiO₂-NPs for 24 h, whereas the expression of total p53 was not changed. Meanwhile, we also found that the SiO₂-NPs lead to the dose-dependent expression of p21 and Gadd45, which were the downstream proteins of p53 in regulating the cell cycle (Figure 10, D and E). It is generally believed that oxidative stress activates multiple signaling pathways, including the p53 signal transduction pathway.⁴⁰ In response to cellular damage, p53 is of importance in genomic surveillance by monitoring the genomic instability.⁴¹ As a cell cycle checkpoint protein, the activation of p53 might result in G2/M delay to allow DNA repair before replication or mitosis, through the expression of p21 and Gadd45. P53, bax, and bcl-2 are also mostly thought to be involved in mitochondria-dependent apoptosis. In the present study, PC12 cells exposed to SiO₂-NPs had an increased expression of bax, while the expression of bcl-2 was equally decreased. A number of studies indicated that the change of bax/bcl-2 ratio could result in significant activation of caspases and then induce apoptosis.⁴² Based on the evidence from our study, the following SiO₂-NP-mediated signaling pathway for cell cycle and apoptosis-related events is proposed: exposure to SiO₂-NPs–ROS production–p53 activation–p21, Gadd45, and bax upregulation/bcl-2 downregulation–G2/M phase arrest and apoptosis.

It is noteworthy in our current study that there were drastic effects on oxidative stress and protein analyses,

but the cellular viability was only moderate. Ueda *et al.*⁴³ have reported that oxidative stress and changes in proteins including JNK, p53, bcl-2, and bax are the early and upstream events in apoptosis; therefore, we postulate that obvious changes in oxidative stress and related proteins might not synchronize with cell death.

Effects of SiO₂-NPs on DA Secretion and Expression Changes of Dopaminergic System-Related Proteins in PC12 Cells. The results obtained from the *in vivo* study indicated that the exposure to SiO₂-NPs resulted in a DA decrease in the striatum (Figure 8A). Consistent with the *in vivo* evidence, the results of the *in vitro* study revealed an obvious dose-dependent decrease in the levels of DA as a result of exposure to SiO₂-NPs (Figure 11A). The decrease in the content of DA may be attributed to the redundant ROS generation in the cells (Figure 9E). It has been shown that the increased ROS levels caused by manganese oxide (Mn-40 nm) particles may participate in the DA depletion in PC12 cells.²⁰ Furthermore, we selected three proteins [tyrosine hydroxylase (TH), dopamine transporter (DAT), and vesicular monoamine transporter 2 (VMAT2)] as indicators for the DA secretion status to investigate the mechanism of decrease in the DA production. TH is the step-limited enzyme of DA synthesis and metabolism.⁴⁴ DAT is a plasma membrane transporter and responsible for the translocation of DA, and VMAT2 has been proposed to be associated with DA storage in synaptic vesicles. The levels of DA in the brain are under a tight and concerted control of DAT, which terminates DA action by removing it from the synaptic cleft, and VMAT2, which packages DA for subsequent release.⁴⁵ The results of the present study indicated that the SiO₂-NPs upregulated the expression of TH in dose-dependent

patterns (Figure 11, B and C). Surprisingly, the SiO_2 -NPs did not alter the expression of VMAT2 or DAT after a 24 h treatment (Figure 11, B and C). These results suggest that the synthesis of DA is the main target function after exposure to SiO_2 -NPs. The dopamine transport system, amazingly, was not significantly affected by the treatment.

CONCLUSION

The results of the present study show a distinct profile of the *in vivo* biodistribution of SiO_2 -NPs in the brain, especially their deposition in the striatum except the olfactory bulb. Such an accumulation could result in oxidative stress, inflammation changes, and functional damage of the striatum. The results of the *in vitro* studies on dopaminergic neurons have demonstrated that SiO_2 -NPs possess remarkable cytotoxic effects and oxidative stress activity against PC12 cells.

Furthermore, the activation of the p53 pathway is involved in mechanistic pathways of the SiO_2 -NP-induced G2/M arrest and apoptosis. Additionally, the decrease in DA levels is most likely attributable to the reduction of DA synthesis. At the current research level of toxicology, the extrapolation of the animals' doses to a human exposure level remains a challenge, since different species may respond differently to the same substance. However, our results of the neurotoxic effect on rat brains could be considered as a suggestion for human exposure level. In summary, these results of the present study imply that there is the potential neurotoxicity of SiO_2 -NPs and a possible risk for neurodegenerative disorders, associated with the exposure to a certain dosage and/or time period. Further investigations are required to assess motor and memory functions through open field tests and the water maze test, respectively.

MATERIALS AND METHODS

General Experimental Design. As shown in Figure 1, a systematic method was devised to assess the biodistribution and potential toxicity of SiO_2 -NPs in the brain *in vivo* and *in vitro*. Accordingly, for the implementation of *in vivo* studies, we have (1) assessed the time-cumulation translocation of intranasal instillation with SiO_2 -NPs into the rat brains and (2) evaluated the responses of oxidative stress, inflammation, and function of rat brain tissues. The results were used as a reference for cell selection in the *in vitro* research. The biological end points displayed in Figure 1 for the *in vitro* work were (1) cell morphology and cytotoxicity; (2) oxidative stress; (3) apoptosis and cell cycle; (4) DA content; and (5) relative molecular mechanisms.

In Vivo Studies

Characterization and Dispersion of SiO_2 -NPs. SiO_2 -NPs were purchased from Sigma Chemical Company (Saint Louis, MO, USA) at $\geq 99.0\%$ purity. The diameter of the particles was confirmed by transmission electron microscopy (TEM, JEM-2010, JEOL Ltd., Tokyo, Japan), and the average particle size was analyzed for 100 particles by Image-pro-plus 5.0 software. For the *in vivo* studies, a SiO_2 -NP stock solution was prepared at a concentration of 1 mg/mL in physiological saline; for the *in vitro* studies, SiO_2 -NPs were suspended at doses ranging from 25 to 200 $\mu\text{g}/\text{mL}$ in high-glucose DMEM (Gibco-Invitrogen Company, Paisley, UK) containing 10% FBS (Gibco-Invitrogen Co.), 100 U/mL penicillin (Gibco-Invitrogen Co.), 100 $\mu\text{g}/\text{mL}$ streptomycin (Gibco-Invitrogen Co.), and 50 ng/mL nerve growth factor (NGF-2.5S, Sigma Chemical Company, Saint Louis, MO, USA). In order to improve the dispersion of nanoparticles in these fluids, the nanoparticle suspension was sonicated with a Hilscher UP200S (Hilscher Ultrasonics GmbH, Teltow, Germany), which generates ultrasonic pulses of 600 W at 20 kHz for 30 min. The size of the nanoparticles and agglomerates and charge measurements in physiological saline or high-glucose Dulbecco's modified Eagle's medium (DMEM) including 10% fetal bovine serum (FBS) were determined with dynamic light scattering and zeta potential measurements using ZetaSizer (Malvern Instruments Ltd., Worcestershire, UK) at a concentration of 1 mg/mL. All the analyzed measurements were obtained for at least three different spots or three times to provide consistency of the data.

Radiolabeling of SiO_2 -NPs with ^{125}I . Radiolabeling of SiO_2 -NPs with ^{125}I was based on a protocol adapted from Xie *et al.*¹¹ Briefly, in order to accomplish the radiolabeling, the SiO_2 -NPs were modified with aminopropyltriethoxysilane to introduce

amino groups onto the surface. The modified SiO_2 -NPs were then incubated with Bolton-Hunter (BH) reagent, dimethylformamide, and Na^{125}I in chloramine. The reaction was terminated by addition of borate buffer supplemented with glycine. Lastly, the ^{125}I labeled SiO_2 -NPs (^{125}I - SiO_2 -NPs) were separated by a column chromatography and were characterized respectively by TEM (JEM-2010, JEOL Ltd., Tokyo, Japan) and Fourier transform infrared (FTIR) spectroscopy (EQUINOX 55, Bruker Co., Germany). The characterization of size and zeta potential of the nanoparticles in physiological saline was performed using ZetaSizer (Malvern Instruments Ltd., Worcestershire, UK).

To identify ^{125}I - SiO_2 -NPs, the resulting solution was extracted and subjected to ITLC-SG and a γ -counter (Shanghai Institute of Nuclear Instrument Factory, China) to assess the radioactive substance. Before the *in vivo* assay, the stability of the ^{125}I - SiO_2 -NPs was analyzed *in vitro*. Briefly, the ^{125}I - SiO_2 -NPs were dissolved in physiological saline containing 10% (vol %) rat serum and incubated at 37 °C. At five time points (1, 3, 7, 15, and 30 days), 2 μL of ^{125}I - SiO_2 -NP suspension was extracted and analyzed by paper chromatography using ITLC-SG. The stability of the ^{125}I - SiO_2 -NPs was expressed as the percentage of radioactivity at the site of ^{125}I - SiO_2 -NPs compared with the total radioactivity.

Protein Adsorption. Rat blood was collected from the orbital venous plexus, under light anesthesia with ether. Serum samples were separated by centrifugation at 8000 rpm for 15 min and stored at -20 °C until assayed. One milligram of SiO_2 -NPs and ^{125}I - SiO_2 -NPs was incubated in 1 mL of phosphate-buffered saline (pH 7.4) with 10% rat serum at 37 °C for 2 h with continuous shaking. After incubation, unbound proteins were separated by a simple centrifugation process (Thermo Shandon, Pittsburgh, PA) at 50000g for 40 min at 4 °C.⁴⁷ Particle pellets were carefully washed four times in the buffer, and the adsorbed protein on each sample was eluted with 1.0 mL of 2% sodium dodecyl sulfate (SDS) solution for 6 h.^{50,51} Afterward, the amount of protein in the SDS solution was quantified by BCA protein assay as described in the manual (Pierce, Rockford, IL, USA).

Animals and Treatment. The animal study was approved by the Animal Ethics Committee of Shanghai Jiaotong University (China). Male SD rats (4 weeks old), weighing approximately 200 g, were purchased from SLACCAS Laboratory Animal Co., Ltd. (Shanghai, China). One week prior to the beginning of the experiment, the rats were housed in pairs under controlled environmental conditions (temperature 23 ± 0.5 °C, humidity $50 \pm 5\%$, lights on 07:00–19:00 h). Rodent diet and water were provided *ad libitum*.

We first evaluated the translocation and distribution of intranasal instillation with ^{125}I -SiO₂-NPs in the rat brain; second we evaluated the general behavior of rats, antioxidative and immune responses, and neurotransmitter content. Consequently, two separate animal experiments were carried out. The animals (six rats per group for each time point) were used for determining SiO₂-NP content in different sub-brain regions (olfactory bulb, striatum, hippocampus, frontal cortex, cerebellum, and brain stem) after intranasal instilling with the SiO₂-NPs for different intervals. The second experiment (12 rats per group) was designed for assessing the general behavior of the rats and other end points described below in the striatum and hippocampus. In the second experiments, the control groups were exposed to the same light anesthesia and were instilled with 10 μL of physiological saline.

Evaluation of Brain Localization. We divided the rats into two groups: (1) intranasal instillation 1 time per day for 1 day; (2) intranasal instillation 1 time per day for 7 days. Under light sodium pentobarbital anesthesia, we instilled 10 μg (10 μL) of ^{125}I -SiO₂-NPs intranasally to each nostril (a total of 20 μg) of the rats held in supine position using a microsyringe once a day and at postinstillation time points of 1 day and 7 days (*i.e.*, 1 day after 1 and 7 times for instillation, respectively); six rats per group were sacrificed. The samples of sub-brain regions were harvested, weighed, and counted for 10 min in a γ -counter to detect the samples' radioactivity.

Animal Behavior Observation. The individual behavioral reaction to administration of SiO₂-NPs or vehicle was assessed. Every animal was monitored for general behavior including gait, posture, and locomotor activity during the experimental period under free behavior conditions.

Oxidative-Stress-Related Biomarker Assay. As the striatum and hippocampus are the major accumulation areas besides the olfactory bulb, we focused the study on injuries occurred in these two regions. The six striatum and hippocampus tissues per group (including the SiO₂-NPs instilled group and the control group) were weighed, and cold protein lysis buffer (50 mM Tris pH 7.4, 150 mM NaCl, 1 mM EDTA, 1 mM EGTA, 5% 2-mercaptoethanol, 1% NP-40, 0.25% sodium deoxycholate, 5 $\mu\text{g}/\text{mL}$ leupeptin, 5 $\mu\text{g}/\text{mL}$ aprotinin, 10 $\mu\text{g}/\text{mL}$ soybean trypsin inhibitor, and 0.2 mM phenylmethyl sulfonylfluoride) was added at the ratio of 1:9 (v/v); the mixtures were homogenized by an ultrasonic cell disruptor (Sonics vibra cell, VCX105) four times, each for 5 s, at 4 °C. The solution was then centrifuged at 14000g at 4 °C for 15 min. The supernatants were collected for analyzing oxidative biomarkers. The activities of GSH and SOD and levels of H₂O₂ and MDA in the striatum and hippocampus extracts were examined. All commercial colorimetric assay kits were purchased from Beyotime Biotech (Nantong, China), and the assays were performed according to manufacturers' instructions.

Measurement of Cytokines. TNF- α , IL-1 β , and IL-8 in the striatum and hippocampus after treatment with SiO₂-NPs and physiological saline for different intervals were measured by an enzyme linked immunosorbent assay (ELISA) kit that is specific for rats (R&D Systems, Oxford, UK). The assays were performed following the manufacturer's instructions. Photometric measurements were conducted at 450 nm using an ELISA reader (Labsystems Dragon Wellscan MK3, Finland).

Histopathological Examination. After exposure for 7 d, the brains were harvested and immediately fixed in a 10% formalin solution. The histopathological tests were performed using standard laboratory procedures. Briefly, the tissues were embedded in paraffin blocks, sectioned into 5 μm slices, and then mounted onto glass slides. After hematoxylin-eosin (HE) staining, the sections were evaluated and photos were taken using an optical microscope. The identity and analysis of the pathology sections were blind to the pathologist.

Assay for Neurotransmitters by a High-Performance Liquid Chromatography System. DA levels in the striatum and Glu levels in the hippocampus were measured by a Waters Alliance HPLC 2695 System (Waters Alliance, Milford, MA). Briefly, the stock solutions of DA and Glu were diluted to appropriate concentrations for the construction of calibration curves, which was established by plotting the mean peak areas *versus* the concentration of

standards. The striatum and hippocampus tissues from rat brains were removed, respectively, weighed, and pooled in 1.5 mL of chilled homogenization buffer (0.1 M citric acid, 0.1 M sodium dihydrogen phosphate monohydrate, 5.6 mM octane sulfonic acid, 10 μM EDTA in 10% (v/v) methanol solution, pH 2.8 with 4 M NaOH). Each sample was sonicated for 20 s (Sonoplus, Bandelin) and centrifuged at 12 000 rpm for 20 min at 4 °C, and the supernatant was analyzed by HPLC.

In Vitro Studies

PC12 Cell Culture Treatment with SiO₂-NPs. The PC12 cell line was obtained from the Cell Bank of Type Culture Collection of Chinese Academy of Sciences in Shanghai. The cells were grown in high-glucose DMEM containing 10% FBS, 100 U/mL penicillin, 100 $\mu\text{g}/\text{mL}$ streptomycin, and 50 ng/mL nerve growth factor at 37 °C in an atmosphere of 5% CO₂.

The SiO₂-NPs were sterilized by heating to 120 °C for 2 h and suspended in the culture medium. The stock solution was then diluted serially to yield doses ranging from 25 to 200 $\mu\text{g}/\text{mL}$. These samples were sonicated for at least 30 min before exposure to the cells to produce a less-aggregated and uniform suspension. After cells had been attached for 24 h in the full medium, the freshly dispersed SiO₂-NP suspensions were immediately applied to the cells. Cells free of SiO₂-NPs were used as the control throughout each *in vitro* assay.

Cell Morphology. PC12 cells were seeded into a six-well plate at a density of 5.0×10^5 cells per well, and different concentrations of SiO₂-NPs were added to the cultures. After 24 h incubation, the cells were washed in ice-cold phosphate-buffered saline (PBS), and cell morphology was assessed with a phase-contrast microscope.

MTS Assay and LDH Measurement. Mitochondrial function and cell viability of the PC12 cells cultured in the media containing different concentrations of SiO₂-NPs (25, 50, 100, and 200 $\mu\text{g}/\text{mL}$) were measured by the MTS assay (CellTiter 96 Assay kit, Promega, Madison, WI, USA). The mechanism is that metabolically active cells will react with a tetrazolium salt in the MTS reagent to produce a soluble formazan dye that can be absorbed at 490 nm. Briefly, cells were plated into a 96-well plate at a density of 2×10^4 cells per well and treated with culture media containing different concentrations of SiO₂-NPs for 24 h. After being incubated with the MTS reagent for 4 h, the plate was read at 490 nm using an ELISA reader (Labsystems Dragon Wellscan MK3, Finland) for optical density. The survival rate of each dose was calculated from the relative absorbance at 490 nm and expressed as the percentage of the control.

The LDH leakage is based on the measurement of LDH activity in the extracellular medium. Following the exposure to SiO₂-NPs for 24 h, the culture medium was aspirated and centrifuged at 3000 rpm for 5 min in order to obtain a cell-free supernatant. The activity of LDH in the medium was determined using a commercial LDH kit (Jiancheng, Nanjing, China) according to the manufacturer's protocols, and the absorption was measured using a UV-visible spectrophotometer (TianMei UV-8500, Shanghai, China) at 440 nm.

Intracellular ROS Measurement and Oxidative Damage. The production of intracellular ROS was measured using the fluorescent probe 2',7'-dichlorofluorescein diacetate (DCFH-DA). DCFH-DA enters the cells passively, where it reacts with ROS to form a highly fluorescent compound, dichlorofluorescein (DCF). Briefly, a DCFH-DA stock solution (10 mM in methanol, Beyotime Biotech, Nantong, China) was diluted 1000-fold in DMEM without serum to yield a 10 μM working solution. PC12 cells were seeded at a density of 5.0×10^5 cells per well in six-well plates. After 6 h exposure to SiO₂-NPs at concentrations of 25, 50, 100, and 200 $\mu\text{g}/\text{mL}$, the cells were incubated in 2 mL of working solution of DCFH-DA at 37 °C for 30 min. The fluorescence was then determined in a flow cytometer (Becton Dickinson, San Jose, CA, USA).

The levels of GSH, SOD, and MDA were respectively measured using the reagent kits (Beyotime Biotech, Nantong, China). Briefly, PC12 cells were plated into six-well plates at a density of 5.0×10^5 cells per well and treated with the SiO₂-NP suspensions. After a 24-h treatment with the SiO₂-NPs, the intracellular levels of GSH, SOD, and MDA were measured, respectively, using the reagent kits according to the manufacturers' instructions.

Measurements of Apoptosis and Cell Cycle. Apoptosis in the PC12 cells was measured using an annexin V-FITC/propidium iodide (PI) apoptosis detection kit (BD PharMingen, San Jose, CA, USA). Briefly, PC12 cells were plated into a six-well culture plate at a density of 5.0×10^5 cells per well. After exposure to SiO_2 -NPs for 24 h, the cells were washed with PBS three times, trypsinized, and then centrifuged at 1000 rpm. The cell pellet were resuspended in 1× binding buffer and stained with annexin V-FITC as recommended by the manufacturer. Subsequently, these samples were diluted with 1× binding buffer and analyzed with a FACScan flow cytometer (Becton Dickinson, San Jose, CA).

For the cell cycle analysis, PC12 cells were plated into a six-well plate at a density of 5.0×10^5 cells per well. After a 24 h exposure to the SiO_2 -NPs, the cells were collected, fixed, permeabilized with 75% ice-cold ethanol, and stored at 20 °C. The cells were then resuspended in 1 mL of lysis buffer (0.1% Triton X-100, 0.05 mg/mL propidium iodide, and 1 mg/mL RNase A), and after incubation for 30 min at 37 °C, the samples were analyzed using the flow cytometer.

Determination of DA by HPLC. Following the SiO_2 -NP treatment, the PC12 cells were homogenized in 0.2 N perchloric acid (20 wt %/vol) containing an internal standard (3,4-dihydroxybenzylamine; 100 ng/mL). The homogenates were centrifuged at 3000 rpm for 20 min at 4 °C, and the supernatant was removed and filtered through a 0.2 μm filter. Aliquots of 25 μL were inserted into the HPLC system (Waters Alliance HPLC 2695 System, Waters Alliance, Milford, MA). The amount of DA was calculated using the standard curves that were generated in triplicate.

Western Blot Analysis. The PC12 cells were stimulated with 25, 50, 100, and 200 $\mu\text{g}/\text{mL}$ of SiO_2 -NPs for 24 h. After incubation, cells were lysed in ice-cold protein lysis buffer [50 mM Tris pH 7.4, 150 mM NaCl, 1 mM EDTA, 1 mM EGTA, 5% 2-mercaptoethanol, 1% NP-40, 0.1% sodium dodecyl sulfate, 5 $\mu\text{g}/\text{mL}$ leupeptin, 5 $\mu\text{g}/\text{mL}$ aprotinin, 10 $\mu\text{g}/\text{mL}$ soybean trypsin inhibitor, and 0.2 mM phenylmethyl sulfonylfluoride] for 30 min. For the evaluation of protein phosphorylation, the same buffer plus phosphatase inhibitor cocktail (Sigma, St. Louis, MO, USA) was used. After centrifuging the lysates at 12 000 rpm at 4 °C for 10 min, the supernatants were collected and stored at –80 °C until used. The protein concentrations were determined with the BCA method (Pierce, Rockford, IL, USA). Proteins of 30 to 50 μg were separated by sodium dodecyl sulfate–polyacrylamide gel electrophoresis (SDS-PAGE) and electrophoretically transferred to polyvinylidene difluoride (PVDF) membranes (Millipore, U.S.). After blocking with 5% nonfat milk in Tris-buffered saline (TBS) containing 0.05% Tween-20 (TBST) for 1 h at room temperature, the membranes were incubated with anti p53, p21, Gadd45, β -actin (Santa Cruz Biotechnology, Santa Cruz, CA, USA), p-p53 (Cell Signaling Technology, Beverly, MA, USA), bax, bcl-2 (Bioworld Technology Inc., USA), TH, DAT, and VMAT2 (Sigma Chemical Company, Saint Louis, MO, USA) overnight at 4 °C. The membranes were then washed with TBST and incubated with a horseradish peroxidase-conjugated anti-rabbit or anti-mouse IgG (Cell Signaling Technology, Beverly, MA, USA) secondary antibody for 1 h at 37 °C, using an enhanced chemiluminescence kit (Millipore, USA). Bio-Rad Quantity One software (Bio-Rad, Richmond, CA, USA) was used to perform the densitometric scanning.

Data Analysis. Data were expressed as mean and standard deviation. Statistical analyses were performed by SPSS 12.0 software, and statistical comparisons were analyzed using the *t* test and one way ANOVA followed by Tukey's HSD *post hoc* test. Differences were considered statistically significant when the *p*-value was less than 0.05.

Acknowledgment. This work was supported by grants from Natural Science Foundation of China (nos. 30870680, 31070843, and 30470479), Shanghai Leading Academic Discipline Project (no. S30206), and Shanghai Sci-Tech Committee Foundation (0752 nm026).

Supporting Information Available: This material is available free of charge via the Internet at <http://pubs.acs.org>.

REFERENCES AND NOTES

- Hirsch, L. R.; Stafford, R. J.; Bankson, J. A.; Sershen, S. R.; Rivera, B.; Price, R. E.; Hazle, J. D.; Halas, N. J.; West, J. L. Nanoshell-Mediated Near-Infrared Thermal Therapy of Tumors under Magnetic Resonance Guidance. *Proc Natl Acad Sci. U. S. A.* **2003**, *23*, 13549–13554.
- Bharali, D. J.; Klejbor, I.; Stachowiak, E. K.; Dutta, P.; Roy, I.; Kaur, N.; Bergey, E. J.; Prasad, P. N.; Stachowiak, M. K. Organically Modified Silica Nanoparticles: A Nonviral Vector for *In Vivo* Gene Delivery and Expression in the Brain. *Proc Natl Acad Sci. U. S. A.* **2005**, *32*, 11539–11544.
- Slowing, I. I.; Trewyn, B. G.; Lin, V. S. Y. Mesoporous Silica Nanoparticles for Intracellular Delivery of Membrane-Impermeable Proteins. *J. Am. Chem. Soc.* **2007**, *28*, 8845–8849.
- Bottini, M.; D'Annibale, F.; Magrini, A.; Cerignoli, F.; Arimura, Y.; Dawson, M. I.; Bergamaschi, E.; Rosato, N.; Bergamaschi, A.; Mustelin, T. Quantum Dot-Doped Silica Nanoparticles as Probes for Targeting of T-lymphocytes. *Int. J. Nanomed.* **2007**, *2*, 227–233.
- Lin, W. S.; Huang, Y. W.; Zhou, X. D.; Ma, Y. F. *In Vitro* Toxicity of Silica Nanoparticles in Human Lung Cancer Cells. *Toxicol. Appl. Pharmacol.* **2006**, *3*, 252–259.
- Park, E. J.; Park, K. Oxidative Stress and Pro-Inflammatory Responses Induced by Silica Nanoparticles *In Vivo* and *In Vitro*. *Toxicol. Lett.* **2009**, *1*, 18–25.
- Wang, J. J.; Sanderson, B. J. S.; Wang, H. Cytotoxicity and Genotoxicity of Ultrafine Crystalline SiO_2 Particulate in Cultured Human Lymphoblastoid Cells. *Environ. Mol. Mutagen.* **2007**, *2*, 151–157.
- Liu, X.; Sun, J. Endothelial Cells Dysfunction Induced by Silica Nanoparticles Through Oxidative Stress via JNK/P53 and NF- κ B Pathways. *Biomaterials* **2010**, *32*, 8198–209.
- Choi, J.; Zheng, Q. D.; Katz, H. E.; Guijarro, T. R. Silica-Based Nanoparticle Uptake and Cellular Response by Primary Microglia. *Environ. Health Perspect.* **2010**, *5*, 589–595.
- Kaewamatawong, T.; Shimada, A.; Okajima, M.; Inoue, H.; Morita, T.; Inoue, K.; Takano, H. Acute and Subacute Pulmonary Toxicity of Low Dose of Ultrafine Colloidal Silica Particles in Mice after Intratracheal Instillation. *Toxicol. Pathol.* **2006**, *7*, 958–965.
- Xie, G.; Sun, J.; Zhong, G.; Shi, L.; Zhang, D. Biodistribution and Toxicity of Intravenously Administered Silica Nanoparticles in Mice. *Arch. Toxicol.* **2010**, *3*, 183–190.
- Yang, R. H.; Chang, L. W.; Wu, J. P.; Tsai, M. H.; Wang, H. J.; Kuo, Y. C.; Yeh, T. K.; Yang, C. S.; Lin, P. Persistent Tissue Kinetics and Redistribution of Nanoparticles, Quantum Dot 705, in Mice: ICP-MS Quantitative Assessment. *Environ. Health Perspect.* **2007**, *9*, 1339–1343.
- Yang, S. T.; Guo, W.; Lin, Y.; Deng, X. Y.; Wang, H. F.; Sun, H. F.; Liu, Y. F.; Wang, X.; Wang, W.; Chen, M.; et al. Biodistribution of Pristine Single-Walled Carbon Nanotubes *In Vivo*. *J. Phys. Chem. C* **2007**, *48*, 17761–17764.
- Wang, J. X.; Liu, Y.; Jiao, F.; Lao, F.; Li, W.; Gu, Y. Q.; Li, Y. F.; Ge, C. C.; Zhou, G. Q.; Li, B.; et al. Time-Dependent Translocation and Potential Impairment on Central Nervous System by Intranasally Instilled TiO_2 Nanoparticles. *Toxicology* **2008**, *1–2*, 82–90.
- Elder, A.; Gelein, R.; Silva, V.; Feikert, T.; Opanashuk, L.; Carter, J.; Potter, R.; Maynard, A.; Finkelstein, J.; Oberdorster, G. Translocation of Inhaled Ultrafine Manganese Oxide Particles to the Central Nervous System. *Environ. Health Perspect.* **2006**, *8*, 1172–1178.
- Wang, B.; Feng, W. Y.; Zhu, M. T.; Wang, Y.; Wang, M.; Gu, Y. Q.; Ouyang, H.; Wang, H. J.; Li, M.; Zhao, Y. L.; et al. Neurotoxicity of Low-Dose Repeatedly Intranasal Instillation of Nano- and Submicron-Sized Ferric Oxide Particles in Mice. *J. Nanopart. Res.* **2009**, *1*, 41–53.
- Tin Tin Win, S.; Yamamoto, S.; Ahmed, S.; Kakeyama, M.; Kobayashi, T.; Fujimaki, H. Brain Cytokine and Chemokine mRNA Expression in Mice Induced by Intranasal Instillation with Ultrafine Carbon Black. *Toxicol. Lett.* **2006**, *2*, 153–160.
- Pettmann, B.; Henderson, C. E. Neuronal Cell Death. *Neuron* **1998**, *4*, 633–647.

19. Pisanic, T. R.; Blackwell, J. D.; Shubayev, V. I.; Finones, R. R.; Jin, S. Nanotoxicity of Iron Oxide Nanoparticle Internalization in Growing Neurons. *Biomaterials* **2007**, *26*, 2572–2581.
20. Hussain, S. M.; Javorina, A. K.; Schrand, A. M.; Duhart, H. M.; Ali, S. F.; Schlager, J. J. The Interaction of Manganese Nanoparticles with PC-12 Cells Induces Dopamine Depletion. *Toxicol. Sci.* **2006**, *2*, 456–463.
21. Ishima, T.; Nishimura, T.; Iyo, M.; Hashimoto, K. Potentiation of Nerve Growth Factor-Induced Neurite Outgrowth in PC12 Cells by Donepezil: Role of Sigma-1 Receptors and IP3 Receptors. *Prog. Neuro-Psychoph.* **2008**, *7*, 1656–1659.
22. Zook, J. M.; Maccuspie, R. I.; Locascio, L. E.; Halter, M. D.; Elliott, J. T. Stable Nanoparticle Aggregates/Agglomerates of Different Sizes and the Effect of Their Size on Hemolytic Cytotoxicity. *Nanotoxicity* **2010**, doi:10.3109/17435390.2010.536615.
23. Bae, E.; Park, H. J.; Lee, J.; Kim, Y.; Yoon, J.; Park, K.; Choi, K.; Yi, J. Bacterial Cytotoxicity of the Silver Nanoparticle Related to Physicochemical Metrics and Agglomeration Properties. *Environ. Toxicol. Chem.* **2010**, *10*, 2154–2160.
24. Lee, J. K. Toxicity and Tissue Distribution of Magnetic Nanoparticles in Mice (2006, vol 89, p 338). *Toxicol. Sci.* **2006**, *1*, 267–267.
25. Fabian, E.; Landsiedel, R.; Ma-Hock, L.; Wiench, K.; Wohlleben, W.; van Ravenzwaay, B. Tissue Distribution and Toxicity of Intravenously Administered Titanium Dioxide Nanoparticles in Rats. *Arch. Toxicol.* **2008**, *3*, 151–157.
26. Marquis, B. J.; Love, S. A.; Braun, K. L.; Haynes, C. L. Analytical Methods to Assess Nanoparticle Toxicity. *Analyst* **2009**, *3*, 425–439.
27. Li, S. D.; Huang, L. Pharmacokinetics and Biodistribution of Nanoparticles. *Mol. Pharma* **2008**, *4*, 496–504.
28. Huot, P.; Levesque, M.; Parent, A. The Fate of Striatal Dopaminergic Neurons in Parkinson's Disease and Huntington's Chorea. *Brain* **2007**, *130*, 222–232.
29. Laakso, M. P.; Lehtovirta, M.; Partanen, K.; Riekkinen, P. J.; Soininen, H. Hippocampus in Alzheimer's Disease: A 3-year Follow-Up MRI Study. *Biol. Psychiat.* **2000**, *6*, 557–561.
30. Wang, J. X.; Zhou, G. Q.; Chen, C. Y.; Yu, H. W.; Wang, T. C.; Ma, Y. M.; Jia, G.; Gao, Y. X.; Li, B.; Sun, J.; et al. Acute Toxicity and Biodistribution of Different Sized Titanium Dioxide Particles in Mice after Oral Administration. *Toxicol. Lett.* **2007**, *2*, 176–185.
31. Nguyen, H. X.; O'Barr, T. J.; Anderson, A. J. Polymorphonuclear Leukocytes Promote Neurotoxicity through Release of Matrix Metalloproteinases, Reactive Oxygen Species, and TNF-alpha. *J. Neurochem.* **2007**, *3*, 900–912.
32. Block, M. L.; Zecca, L.; Hong, J. S. Microglia-Mediated Neurotoxicity: Uncovering the Molecular Mechanisms. *Nat. Rev. Neurosci.* **2007**, *8*, 57–69.
33. Tansey, M. G.; Frank-Cannon, T. C.; McCoy, M. K.; Lee, J. K.; Martinez, T. N.; McAlpine, F. E.; Ruhn, K. A.; Tran, T. A. Neuroinflammation in Parkinson's Disease: Is There Sufficient Evidence for Mechanism-Based Interventional Therapy? *Front. Biosci.* **2008**, *13*, 709–717.
34. AshaRani, P. V.; Mun, G. L. K.; Hande, M. P.; Valiyaveettil, S. Cytotoxicity and Genotoxicity of Silver Nanoparticles in Human Cells. *ACS Nano* **2009**, *2*, 279–290.
35. Nel, A.; Xia, T.; Madler, L.; Li, N. Toxic Potential of Materials at the Nanolevel. *Science* **2006**, *5761*, 622–627.
36. Cui, K.; Luo, X. L.; Xu, K. Y.; Murthy, M. R. V. Role of Oxidative Stress in Neurodegeneration: Recent Developments in Assay Methods for Oxidative Stress and Nutraceutical Antioxidants. *Prog. Neuro-Psychoph.* **2004**, *5*, 771–799.
37. Perluigi, M.; Sultana, R.; Cenini, G.; Di Domenico, F.; Memo, M.; Pierce, W. M.; Coccia, R.; Butterfield, D. A. Redox Proteomics Identification of 4-hydroxyxenonol-modified Brain Proteins in Alzheimer's Disease: Role of Lipid Peroxidation in Alzheimer's Disease Pathogenesis. *Proteom. Clin. Appl.* **2009**, *6*, 682–693.
38. Mates, J. M.; Perez-Gomez, C.; De Castro, I. N. Antioxidant Enzymes and Human Diseases. *Clin. Biochem.* **1999**, *8*, 595–603.
39. Singh, N.; Manshian, B.; Jenkins, G. J. S.; Griffiths, S. M.; Williams, P. M.; Maffei, T. G. G.; Wright, C. J.; Doak, S. H. NanoGenotoxicology: The DNA Damaging Potential of Engineered Nanomaterials. *Biomaterials* **2009**, *23*–24, 3891–3914.
40. Circu, M. L.; Aw, T. Y. Reactive Oxygen Species, Cellular Redox Systems, and Apoptosis. *Free Radical Biol. Med.* **2010**, *6*, 749–762.
41. Liu, Y. P.; Lin, Y.; Ng, M. L. Immunochemical and Genetic Analysis of the p53 Gene in Liver Preneoplastic Nodules from Aflatoxin-Induced Rats in One Year. *Ann. Acad. Med. Singapore* **1996**, *1*, 31–36.
42. Huang, J.; Wu, L. J.; Tashiro, S.; Onodera, S.; Ikejima, T. Bcl-2 Up-Regulation and P-p53 Down-Regulation Account for the Low Sensitivity of Murine L929 Fibrosarcoma Cells to Oridonin-induced Apoptosis. *Biol. Pharm. Bull.* **2005**, *11*, 2068–2074.
43. Ueda, S.; Masutani, H.; Nakamura, H.; Tanaka, T.; Ueno, M.; Yodoi, J. Redox Control of Cell Death. *Antioxid. Redox Signaling* **2002**, *3*, 405–414.
44. Fornai, F.; Lenzi, P.; Lazzeri, G.; Ferrucci, M.; Fulceri, F.; Giorgi, F. S.; Falleni, A.; Ruggieri, S.; Paparelli, A. Fine Ultrastructure and Biochemistry of PC12 Cells: A Comparative Approach to Understand Neurotoxicity. *Brain Res.* **2007**, *1*, 174–190.
45. Schuh, R. A.; Richardson, J. R.; Gupta, R. K.; Flaws, J. A.; Fiskum, G. Effects of the Organochlorine Pesticide Methoxychlor on Dopamine Metabolites and Transporters in the Mouse Brain. *Neurotoxicology* **2009**, *2*, 274–280.
46. Lin, W.; Huang, Y. W.; Zhou, X. D.; Ma, Y. *In Vitro* Toxicity of Silica Nanoparticles in Human Lung Cancer Cells. *Toxicol. Appl. Pharmacol.* **2006**, *3*, 252–259.
47. Wang, F.; Gao, F.; Lan, M.; Yuan, H.; Huang, Y.; Liu, J. Oxidative Stress Contributes to Silica Nanoparticle-Induced Cytotoxicity in Human Embryonic Kidney Cells. *Toxicol. In Vitro* **2009**, *5*, 808–815.
48. Maurer-Jones, M. A.; Lin, Y. S.; Haynes, C. L. Functional Assessment of Metal Oxide Nanoparticle Toxicity in Immune Cells. *ACS Nano* **2010**, *6*, 3363–3373.
49. Deng, Z. J.; Mortimer, G.; Schiller, T.; Musumeci, A.; Martin, D.; Minchin, R. F. Differential Plasma Protein Binding to Metal Oxide Nanoparticles. *Nanotechnology* **2009**, *45*, 1–9.
50. Zhao, C. S.; Liu, X. D.; Nomizu, M.; Nishi, N. Blood Compatible Aspects of DNA-Modified Polysulfone Membrane-Protein Adsorption and Platelet Adhesion. *Biomaterials* **2003**, *21*, 3747–3755.
51. Takami, Y.; Yamane, S.; Makinouchi, K.; Otsuka, G.; Glueck, J.; Benkowski, R.; Nose, Y. Protein Adsorption onto Ceramic Surfaces. *J. Biomed. Mater. Res.* **1998**, *1*, 24–30.